EXACTLY SOLVABLE POTENTIAL
WITH A PRONOUNCED MAXIMUM

Matti SELG

Institute of Physics of the University of Tartu, Riia 142, 51014 Tartu, Estonia;
matti@fi.tartu.ee

Abstract. An analytic method for solving the one-dimensional Schrödinger equation is applied to confining potentials with well-defined maxima. Exactly solvable substitute for the original potential is constructed, which consists of several smoothly joined Morse-type (ordinary, reversed, or pseudo-Morse) components. The analytic procedures of calculating the complete spectrum of the bound and quasi-bound states as well as the corresponding stationary wavefunctions are described, and an exact formula for the wavefunction's phase shift is derived. The efficacy of the approach is demonstrated on the rotationally highly excited excimers Xe_2^* in the electronic state 0_u^+.

Key words: exactly solvable potentials, quasi-bound states, phase shift.

1. INTRODUCTION

Rigorous methods for solving the quantum-mechanical inverse problem, that is, deducing the interaction potential from the experimental data, have been worked out about 50 years ago, thanks to the remarkable efforts by Marchenko, Gel'fand, Levitan and others (see [1] for a comprehensive review). In spite of this long-stretching history one may even nowadays come upon a misconception, as if a confining potential could be uniquely determined from its complete energy spectrum. Erroneousness of this standpoint was first demonstrated by Bargmann [2,3], who explicitly built up several different potentials having the same energy spectrum and also the same energy dependence of the wavefunction's phase shift. Many years later Abraham and Moses [4] elaborated a simple procedure

for constructing isospectral potentials and the relevant normalized wavefunctions. According to their method the new potential is calculated as follows [5]:

$$U(x) = V(x) + 2\frac{d}{dx}\ln\left[1 + \gamma I(x)\right], \tag{1}$$

where $V(x)$ denotes the original potential, γ is a constant, and the function

$$I(x) = \int_{-\infty}^{x} dy\left[\varphi_0(x)\right]^2 \tag{2}$$

is determined by the initial ground-state eigenfunction $\varphi_0(x)$, which in turn transforms to

$$\Psi_0(x) = \varphi_0(x)\frac{\sqrt{1+\gamma}}{1+\gamma I(x)}. \tag{3}$$

Thus the new potential (1) and the "renormalized" ground-state wavefunction (3) are both related to the parameter γ, which generates a family of isospectral potentials (and corresponding wavefunctions). In Fig. 1 the Abraham–Moses method is demonstrated for the 0_u^+ state of the excimer Xe_2^*, whose potential parameters have been specified elsewhere [6]. Compared with the original one, the new potential is of essentially different shape only in case of comparatively large values of γ, or alternatively, when $\gamma \to -1$. The latter is just the limit case when the previous zeroth level is removed from the energy spectrum, while the other levels remain in their positions. One can infer that it is not so easy to distinguish the cases $\gamma = 0$ and $\gamma = -1$ when trying to determine the potential on the basis of the available experimental data.

The purpose of the above discussion was to point at a regrettable fact that our knowledge of the actual interaction potential for almost any quantum system to study is more or less incomplete. Although, as mentioned, the strict criteria for the unique solution of the quantum-mechanical inverse problem have been stated long ago; they are usually extremely difficult to fulfil. A rather thriving strategy in this situation is to construct a potential that would take a possibly full account of the available information (experimental and theoretical) about the quantum system, being at the same time exactly solvable. Varying the parameters of such a probe potential and performing the needful quantum-mechanical calculations, one can gradually come closer to the real interaction potential for the system. Of course, such an approach is only justified if one is looking for a reasonable potential in comparatively limited distance and energy ranges, not in the whole physical domain.

Aiming at this goal, the author recently proposed a simple method for constructing exactly solvable substitute potentials with the help of several smoothly joined Morse-type components [7]. As is known, any Morse-type potential induces a Schrödinger equation that can be converted into a confluent hypergeometric equation, which always (not only in the classical Morse case) has the analytic
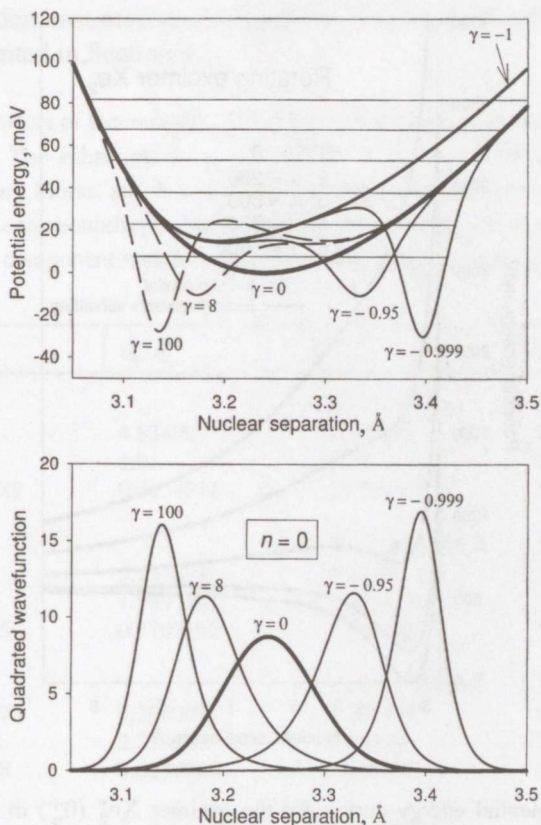
Fig. 1. The Abraham–Moses method [4] is applied to the excimer Xe_2^* in the electronic state 0_u^+. The horizontal lines indicate the vibrational levels of the system (the same for all potentials). The value $\gamma = 0$ corresponds to the original potential. When $\gamma = -1$, the previous zeroth level is removed from the spectrum, while the positions of all other bound states remain unchanged.

solution. Still more recently the same idea has been applied to double-well potentials [8]. In principle, the method can be extended to describe any one-dimensional quantum system in a limited range. For example, it can be applied to a diatomic molecule in an arbitrary rotational substate. This is demonstrated in Fig. 2, where the initial exactly solvable rotationally unexcited potential (curve 1) has already been partially shown in Fig. 1 (the curve with $\gamma = 0$). The exactly solvable substitutes for the effective potentials of the rotationally excited excimers have been determined from the appropriate least squares' fits and their parameters are given in Table 1. One can see that with a relatively small number of components a surprisingly good fit in a reasonably wide distance range can be found for the potentials of rather different shape.
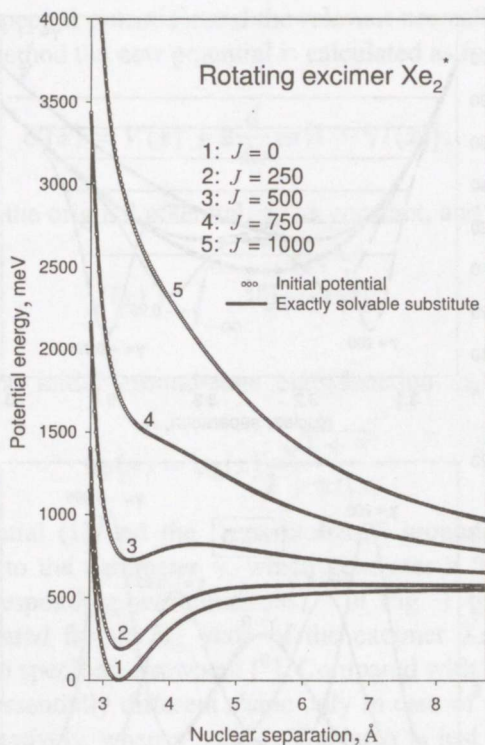
235

Fig. 2. Effective potential energy curves for the excimer Xe_2^* (0_u^+) in different rotational substates. The parameters of the exactly solvable component potentials (solid lines) are given in Table 1.

Fully repulsive (curves 4 and 5 in Fig. 2) and nearly flat (curves 1 and 2) Morse-based potentials have been studied in detail elsewhere [6,7]. Here we only want to point out that these earlier results can be applied to the effective potentials for the rotationally excited diatomic molecules, since any of them can be approximated by a reasonable exactly solvable substitute. From Table 1 one can see that curves 4 and 5 do not entirely consist of Morse-type components: a small part of them is approximated by a straight line. This little complement is needed to ensure the continuity of the potential and its first derivative. It does not affect the exact solvability of the problem, since a linear potential induces an analytic solution in terms of the well-known Airy functions [9].

In this paper we concentrate on the analysis of the potentials having a pronounced hump (like curve 3 in Fig. 2). The most specific feature of this case is a wide metastability range between the dissociation energy and the top of the potential barrier, where instead of the usual vibrational levels one has to take account of the quasi-bound states (resonances). In Section 2 we describe all details of calculating the bound and quasi-bound vibrational levels, the corresponding stationary wavefunctions, and the profiles of the resonances. The results of

calculations are demonstrated and analysed in Section 3. Finally, a conclusion of the work is presented in Section 4.

Table 1. The parameters of the smoothly joined components of the exactly solvable potentials shown in Fig. 2. The subscripts $k = -1$ and $k = 0$ are related to the pseudo-Morse, $k = 1$ to the ordinary Morse, and $k = 2$ to the reversed Morse components, respectively. X_k ($k = 0, 1, 2$) denote the boundary points, and J the rotational quantum number. For $J = 750$ and $J = 1000$, the component with $k = 1$ represents a straight line $U_1(R) = \alpha_1 R + V_1$

k	D_k, meV	α_k, Å^{-1}	R_k, Å	V_k, meV
	$J = 0$		$X_1 = 2.95$ Å	$X_2 = 5.080853$ Å
0	0.186119	4.83408	3.702782	26.9298
1	515.53	1.91	3.24	0
2	−0.0920789	0.4154014	13.080853	551.23
	$J = 250$		$X_1 = 2.926495$ Å	$X_2 = 3.880719$ Å
0	0.214814	5.194871	3.6258	288.9
1	419.3686	1.949744	3.273318	188.4303
2	−6.808495	0.7705152	6.264231	579.8639
	$J = 500$		$X_1 = 3.150787$ Å	$X_2 = 3.836371$ Å
0	0.08647475	3.296007	4.2814727	679.394525
1	151.7572	2.215147	3.414983	725.5279
2	−192.9908	0.6292893	4.431376	821.2128
	$J = 750$	$X_0 = 3.14$ Å	$X_1 = 3.68$ Å	$X_2 = 4.08$ Å
−1	0.0685224	2.933997	4.541099	1581.9275
0	0.0279844	1.875	5.688487	1439.485
1		−206.4243		2248.817
2	−794.6609	0.562215	3.28	1410.872
	$J = 1000$	$X_0 = 3.24$ Å	$X_1 = 3.90$ Å	$X_2 = 4.22$ Å
−1	0.0391075	2.21653	5.301897	2666.993
0	0.0044775	0.75	11.49535	1959.7
1		−611.8529		4740.241
2	−8841.262	0.475161	−1.12	9656.522

2. SOLUTION OF THE SCHRÖDINGER EQUATION

2.1. Model

According to the general idea of the approach [7], the model potential we are going to study consists of three components, as shown in Fig. 3. They all have the well-known analytic form of the Morse potential

$$U_k(R) = V_k + D_k \left[e^{-\alpha_k(R-R_k)} - 1 \right]^2 \qquad (k = 0, 1, 2). \qquad (4)$$
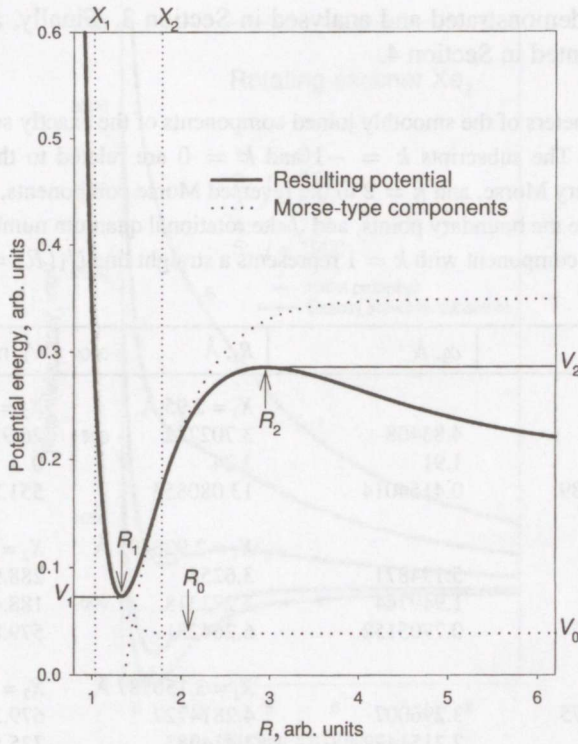
Fig. 3. The model potential analysed in this paper. Notation of the components corresponds to formula (4). Note that, although invisible on the scale of the figure, the pseudo-Morse potential still has a minimum at R_0.

In the short distances' region $R \leq X_1$ ($k = 0$) the potential is approximated by a pseudo-Morse potential $U_0(R)$, whose main peculiarity is that the parameters D_0 and α_0 are not independent, but $D_0 = \hbar^2 \alpha_0^2 / (8m)$ with m being the reduced mass of the particle. It means that the potential well is just of the limit depth when there is no discrete spectrum any more [9]. If needed, one can introduce additional pseudo-Morse components with subscripts $k = -1, -2, -3, \ldots$

The central part of the potential curve $X_1 \leq R \leq X_2$ ($k = 1$) is approximated by an ordinary Morse potential, while the hump's region $R \geq X_2$ ($k = 2$), which we are most interested in, is described by a reversed Morse potential with the parameter D_2 being negative. The same system of notation – subscript $k = 0$ (and $k = -1, -2, -3, \ldots$) for the pseudo-Morse, $k = 1$ for the ordinary Morse, and $k = 2$ for the reversed Morse components – will be used throughout this paper (including Table 1 related to the potentials in Fig. 2).

The solution scheme of the Schrödinger equation is essentially the same as described in Subsection 2.1 of Ref. [7]. The first step is to introduce dimensionless variables for the three distance regions under examination: $y_k \equiv 2a_k \exp(-\alpha_k(R - R_k))$ ($k = 0, 1, 2$), where $a_k = \sqrt{2mD_k}/(\hbar\alpha_k)$ (and

consequently, $a_0 = \frac{1}{2}$). The relevant Schrödinger equations then become

$$\frac{d^2\Psi(y_k)}{dy_k^2} + \frac{1}{y_k}\frac{d\Psi(y_k)}{dy_k} + \left[-\frac{\mu_k^2}{y_k^2} \pm \left(\frac{a_k}{y_k} - \frac{1}{4}\right)\right]\Psi(y_k) = 0 \qquad (k = 1, 2, 3)\,, \quad (5)$$

where the plus sign in square brackets corresponds to the indices $k = 0$ and $k = 1$, and minus to $k = 2$. The quantities μ_k^2 are defined as follows: $\mu_k^2 = (a_k^2/D_k) \cdot (V_k + D_k - E)$, $k = 0, 1, 2$. Note that $D_2 < 0$ and μ_0 is a pure imaginary quantity for any stationary state, since always $E > V_0 + D_0$.

The next traditional step is to convert (5) into the confluent hypergeometric form, using a transformation $\Psi \sim \exp(-x/2)x^c G(b, c; x)$,

$$x\frac{d^2G(b, c; x)}{dx^2} + (2c + 1 - x)\frac{dG(b, c; x)}{dx} + \left(b - c - \frac{1}{2}\right)G(b, c; x) = 0, \quad (6)$$

with the parameters b, c and the dimensionless coordinate x, which for different energy and distance regions are specified in Table 2 ($\beta_k \equiv |\mu_k|$):

Table 2. The quantities related to Eq. (6) in different regions

	$R \leq X_1$ $E \leq V_1 + D_1$	$X_1 \leq R \leq X_2$ $E \geq V_1 + D_1$	$X_1 \leq R \leq X_2$ $E \leq V_1 + D_1$	$R \geq X_2$ $E \leq V_2 + D_2$	$R \geq X_2$ $E \geq V_2 + D_2$
b	$1/2$	a_1	a_1	ia_2	ia_2
c	$i\beta_0$	μ_1	$i\beta_1$	μ_2	$i\beta_2$
x	y_0	y_1	y_1	iy_2	iy_2

The fundamental solution of (6) can be always built up of the special solutions $G_1 \equiv \Psi(-b + c + \frac{1}{2}, 2c + 1; x)$ and $G_2 \equiv \exp(x)\Psi(b + c + \frac{1}{2}, 2c + 1; -x)$ [10], which for sufficiently large x can be evaluated from the asymptotic series

$$\Psi(a, c; x) = x^{-a}\sum_{n=0}^{N}\frac{(a)_n(a - c + 1)_n}{n!(-x)^n}, \quad (7)$$

where $(a)_n \equiv \Gamma(a + n)/\Gamma(a) = a(a + 1)(a + 2)...(a + n - 1)$ is the Pochhammer symbol. This simple formula may not converge for smaller x, directing one to a more complicated but universal expansion

$$\Psi(a, c; x) = \frac{\Gamma(1 - c)}{\Gamma(a + 1 - c)}\Phi(a, c; x) + \frac{\Gamma(c - 1)}{\Gamma(a)}x^{1-c}\Phi(a + 1 - c, 2 - c; x), \quad (8)$$

where the symbols

$$\Phi(a, c; x) = 1 + \frac{a}{c}\frac{x}{1!} + \frac{a(a+1)}{c(c+1)}\frac{x^2}{2!} + \dots \tag{9}$$

denote confluent hypergeometric functions. Equivalently, the general solution of (6) can be directly constructed from $F_1 \equiv \Phi(-b + c + \frac{1}{2}, 2c + 1; x)$ and $F_2 \equiv x^{-2c}\Phi(-b - c + \frac{1}{2}, -2c + 1; x)$.

2.2. Solution in the small distances' region

The general solution of the Schrödinger equation (5) is actually needed only for the central part $X_1 \leq R \leq X_2$ of the potential, while in the regions $R \leq X_1$ and $R \geq X_2$ its form is essentially simplified. For example, as $G_2 \to \infty$ when $x \to \infty$, one immediately gets the solution with the correct asymptotic behaviour (i.e., vanishing at $x \to \infty$) in the region $R \leq X_1$:

$$\Psi_0 \sim \exp(-y_0/2)y_0^{i\beta_0}\Psi(i\beta_0, 2i\beta_0 + 1; y_0).$$

Thereafter, using (8) and noting that $y_0 = \exp(-\alpha(R - R_0))$, one comes to the formula

$$\Psi_0 = N_0 C_0(y_0) \cos[\varphi_0 + D_0(y_0) - \alpha_0\beta_0 R], \tag{10}$$

where N_0 is the normalization factor (i.e., a real constant),

$$C_0(y_0)e^{iD_0(y_0)} \equiv \exp(-y_0/2)\Phi(i\beta_0, 2i\beta_0 + 1; y_0)$$

$$= 1 - \frac{y_0/4}{\beta_0 + \frac{1}{2}} + \frac{(y_0/4)^2}{(\beta_0 + \frac{1}{2})\,1!}\left(1 - \frac{y_0/4}{\beta_0 + \frac{3}{2}}\right)$$

$$+ \frac{(y_0/4)^4}{(\beta_0 + \frac{1}{2})(\beta_0 + \frac{3}{2})\,2!}\left(1 - \frac{y_0/4}{\beta_0 + \frac{5}{2}}\right) + \dots, \tag{11}$$

according to [6], and

$$\varphi_0 \equiv \alpha_0\beta_0 R_0 - \arg[\Gamma(2i\beta_0)/\Gamma(i\beta_0)]. \tag{12}$$

Formula (10) related to a pseudo-Morse potential has been derived in [6]. However, an important innovation here is the explicit expression for the phase shift, which does not contain any additional terms (otherwise the wavefunction would not be real!) and, as we now demonstrate, can be easily evaluated for any given energy. Indeed, using the Legendre formula for doubling a gamma function's argument [10]

$$\Gamma(2z) = \frac{2^{2z-1}}{\sqrt{\pi}}\Gamma(z)\Gamma\left(z + \frac{1}{2}\right) \tag{13}$$

and the formula [11]

$$\arg \Gamma \left(i\gamma + \frac{1}{2} \right) = \gamma \left[\frac{1}{2} \ln(1 + 4\gamma^2) - \ln 2 - 1 \right]$$

$$- \frac{1}{2} \int_0^\infty \left(\coth t - \frac{1}{t} \right) e^{-t} \sin(2\gamma t) \frac{dt}{t}, \tag{14}$$

one can write

$$\arg \left[\Gamma(2i\beta_0)/\Gamma(i\beta_0) \right] = \beta_0 \left[\frac{1}{2} \ln(1 + 4\beta_0^2) - \ln 2 - 1 \right]$$

$$- \frac{1}{2} \int_0^\infty \left(\coth t - \frac{1}{t} \right) e^{-t} \sin(2\beta_0 t) \frac{dt}{t}, \tag{15}$$

which conclusively fixes the phase shift (12) for the wavefunction (10).

Another important quantity for finding the stationary states of the system, the wavefunction's dimensionless logarithmic derivative, then becomes [6]

$$F_0(E, R) \equiv \frac{1}{\alpha_0} \frac{\Psi_0'}{\Psi_0} = \frac{y_0}{2} + \beta_0 \frac{C_{00}(y_0)}{C_0(y_0)} \frac{\sin \left[\varphi_0 + D_{00}(y_0) - \alpha_0 \beta_0 R \right]}{\cos \left[\varphi_0 + D_0(y_0) - \alpha_0 \beta_0 R \right]}, \tag{16}$$

where the function $C_{00}(y_0)e^{iD_{00}(y_0)} \equiv \exp(-y_0/2)\Phi(i\beta_0 + 1, 2i\beta_0 + 1; y_0)$ can be calculated with the help of (11), if one replaces $y_0 \to -y_0$, in accordance with the general relation [10]

$$\exp(-y_0/2)\Phi(i\beta_0 + 1, 2i\beta_0 + 1; y_0) = \exp(y_0/2)\Phi(i\beta_0, 2i\beta_0 + 1; -y_0). \tag{17}$$

2.3. Bound states' region ($E \leq V_2 + D_2$)

In the central region $X_1 \leq R \leq X_2$, as already mentioned, one has to examine the general solution of the Schrödinger equation (5), which is more conveniently expressed in terms of the functions F_1 and F_2 defined in the last paragraph of Subsection 2.1. The corresponding wavefunction then reads

$$\Psi_1 = N_1^{(+)} y_1^{\mu_1} S(a_1, \mu_1; y_1) + N_1^{(-)} y_1^{-\mu_1} S(a_1, -\mu_1; y_1), \quad X_1 \leq R \leq X_2, \tag{18}$$

where $N_1^{(+)}$ and $N_1^{(-)}$ are some real constants and the S-functions

$$S(a, \mu; x) \equiv e^{-x/2} \Phi(-a + \mu + \tfrac{1}{2}, 2\mu + 1; x), \tag{19}$$

according to [7], can be evaluated as follows:

241

$$S(a, \mu; x) = \sum_{n=0}^{\infty} B_n \quad (k = 1, 2) \tag{20}$$

with $B_0 = 1$, $B_1 = -\dfrac{ax}{2\mu + 1}$, $B_n = \dfrac{x}{n(2\mu + n)}\left(-aB_{n-1} + \dfrac{x}{4}B_{n-2}\right)$, $n = 2, 3, \ldots$

The corresponding dimensionless logarithmic derivative then becomes

$$
\begin{aligned}
F_1(E, R) &\equiv \frac{1}{\alpha_1}\frac{\Psi_1'}{\Psi_1} = \frac{y_1 + 1}{2} - a_1 \\
&+ \left(a_1 - \frac{1}{2}\right)\frac{N_1 y_1^{\mu_1} S(a_1 - 1, \mu_1; y_1) + y_1^{-\mu_1} S(a_1 - 1, -\mu_1; y_1)}{N_1 y_1^{\mu_1} S(a_1, \mu_1; y_1) + y_1^{-\mu_1} S(a_1, -\mu_1; y_1)} \\
&- \mu_1 \frac{N_1 y_1^{\mu_1} S(a_1 - 1, \mu_1; y_1) - y_1^{-\mu_1} S(a_1 - 1, -\mu_1; y_1)}{N_1 y_1^{\mu_1} S(a_1, \mu_1; y_1) + y_1^{-\mu_1} S(a_1, -\mu_1; y_1)},
\end{aligned}
\tag{21}
$$

$$N_1 \equiv \frac{N_1^{(+)}}{N_1^{(-)}}.$$

The solution for the right-side region $R \geq X_2$ has been given elsewhere [7], taking into consideration that the F_2-term should be omitted, since $F_2 \to \infty$, when $R \to \infty$ ($y_1 \to 0$). Consequently,

$$\Psi_2 = N_2 y_2^{\mu_2} S(ia_2, \mu_2; iy_2), \ R \geq X_2 \tag{22}$$

with the normalization factor N_2 and the relevant S-function given by (20). The corresponding dimensionless logarithmic derivative reads

$$
\begin{aligned}
F_2(E, R) &\equiv \frac{1}{\alpha_2}\frac{\Psi_2'}{\Psi_2} \\
&= \frac{S(ia_2, \mu_2 + 1; iy_2)y_2^2}{8(\mu_2 + 1)S(ia_2, \mu_2; iy_2)}\left[1 + \frac{a_2^2}{(\mu_2 + \frac{1}{2})^2}\right] - \mu_2 - \frac{a_2 y_2}{2\mu_2 + 1}.
\end{aligned}
\tag{23}
$$

2.4. Eigenstates in the quasi-bound ($V_2 + D_2 \leq E \leq V_2$) and free particles' ($E > V_2$) regions

Differently from the previous case $\mu_k = i\beta_k$ ($k = 1, 2$). It means that formula (18) related to the central region $X_1 \leq R \leq X_2$ transforms into a sum of two complex conjugate terms. The corresponding expressions for the wavefunction and its logarithmic derivative can be taken from [6]:

$$\Psi_{11} = N_{11} C_1(y_1) \cos\left[\varphi_1 + D_1(y_1) - \alpha_1 \beta_1 R\right], \ X_1 \leq R \leq X_2, \tag{24}$$

$$F_{11}(E,R) \equiv \frac{1}{\alpha_1}\frac{\Psi'_{11}}{\Psi_{11}} = \frac{y_1+1}{2} - a_1$$

$$+\left(a_1 - \frac{1}{2}\right)\frac{C_{11}(y_1)\cos(\varphi_1 + D_{11}(y_1) - \alpha_1\beta_1 R)}{C_1(y_1)\cos(\varphi_1 + D_1(y_1) - \alpha_1\beta_1 R)}$$

$$+\beta_1\frac{C_{11}(y_1)\sin(\varphi_1 + D_{11}(y_1) - \alpha_1\beta_1 R)}{C_1(y_1)\cos(\varphi_1 + D_1(y_1) - \alpha_1\beta_1 R)}, \tag{25}$$

where $C_1(y_1)e^{iD_1(y_1)} \equiv S(a_1, i\beta_1; y_1)$, $C_{11}(y_1)e^{iD_{11}(y_1)} \equiv S(a_1 - 1, i\beta_1; y_1)$, N_{11} is the normalization factor and the phase shift φ_1 will be specified in Section 3.

The solution for the region $R \geq X_2$ constructed from the functions F_1 and F_2 again turns to a sum of two complex conjugate terms (see Table 2), and therefore

$$\Psi_{22} = 2C_2(y_2)\cos\left[\varphi_2 + D_2(y_2) - \alpha_2\beta_2 R\right], \ R \geq X_2, \tag{26}$$

with $C_2(y_2)e^{iD_2(y_2)} \equiv S(ia_2, i\beta_2; iy_2)$, φ_2 being the relevant phase shift, and the fixed value of the normalization factor ($N_{22} = 2$) corresponding to the asymptotic normalization of the wavefunctions in the continuous energy spectrum (see [9], Section 21)

$$\int \Psi_p^* \Psi_{p'} dR = 2\pi\hbar\delta(p - p'), \tag{27}$$

where p is the momentum of the particle at infinity.

The wavefunction's dimensionless logarithmic derivative in this region becomes

$$F_{22}(E,R) \equiv \frac{1}{\alpha_2}\frac{\Psi'_{22}}{\Psi_{22}} = \beta_2\tan\delta_2 \cdot \left(1 - \frac{2a_2 y_2}{4\beta_2^2 + 1}\right) - \frac{a_2 y_2}{4\beta_2^2 + 1}$$

$$+ \frac{y_2^2}{8C_2^2(y_2)}\left[A_2 U_2 - B_2 V_2 - \tan\delta_2 \cdot (A_2 V_2 + B_2 U_2)\right], \tag{28}$$

where

$$A_2 \equiv \frac{1}{\beta_2^2 + 1} - \frac{4a_2^2(8\beta_2^2 - 1)}{(\beta_2^2 + 1)(4\beta_2^2 + 1)^2},$$

$$B_2 \equiv \frac{4\beta_2 a_2^2(5 - 4\beta_2^2)}{(\beta_2^2 + 1)(4\beta_2^2 + 1)^2} - \frac{\beta_2}{\beta_2^2 + 1},$$

$$\delta_2 \equiv \varphi_2 + D_2(y_2) - \alpha_2\beta_2 R,$$

$$U_2 \equiv \operatorname{Re} S(ia_2, i\beta_2; iy_2)\operatorname{Re} S(ia_2, i\beta_2 + 1; iy_2)$$

$$+ S(ia_2, i\beta_2; iy_2)\operatorname{Im} S(ia_2, i\beta_2 + 1; iy_2),$$

243

and

$$V_2 \equiv \operatorname{Re} S(ia_2, i\beta_2; iy_2) \times \operatorname{Im} S(ia_2, i\beta_2 + 1; iy_2)$$

$$- \operatorname{Im} S(ia_2, i\beta_2; iy_2) \operatorname{Re} S(ia_2, i\beta_2 + 1; iy_2).$$

3. CALCULATION OF ENERGY EIGENVALUES AND EIGENFUNCTIONS

The bound states can be determined from demand of continuity of the wavefunction's logarithmic derivative at a suitable reference point, for example at $R = X_2$. Indeed, for any given energy E one can evaluate the function $F_2(E, X_2)$ given by (23). On the other hand, one may calculate the logarithmic derivative $F_0(E, X_1)$ according to (16) and then use the continuity condition $F_0(E, X_1) = F_1(E, X_1)$ to fix the constant N_1 in (21). This way one comes to another expression $F_1(E, X_2)$ for the logarithmic derivative at the boundary point X_2. These two independent estimations of the same quantity can only coincide for the true energy eigenvalues $E = E_n$, which means that the quantization equation reduces to the boundary condition

$$F_1(E, X_2) = F_2(E, X_2). \tag{29}$$

Naturally, instead of X_2 one might use any other reference point within the scope for the same purpose.

The success in exploiting Eq. (29) depends on the accuracy of the initial prognoses for the energy levels, which can be made using the Lagrange extrapolation method, as shown elsewhere [7]. The idea is to take account of the already ascertained bound states, and the method works well with just four previous levels (E_0, E_1, E_2, E_3) used to estimate the next one

$$E_4 \approx 4E_3 - 6E_2 + 4E_1 - E_0. \tag{30}$$

The corresponding exact eigenvalue is then easily found by solving Eq. (29) with the help of an appropriate iteration procedure. Having determined the eigenvalue $E = E_n$, one uses the conditions $N_1^{(+)}/N_1^{(-)} = N_1$, $\Psi_0(E_n, X_1) = \Psi_1(E_n, X_1)$, $\Psi_1(E_n, X_2) = \Psi_2(E_n, X_2)$, and $\int_0^\infty [\Psi(E_n, R)]^2 dR = 1$ [where $\Psi(E_n, R)$ is the overall wavefunction] to determine the normalization factors in (10), (18), and (22).

Now, let us concern with the specific features of the quasi-bound eigenstates, which can be described in terms of the quasi-stationary states, adding a small imaginary part to each energy level (see [9], Section 134). However, a more straightforward approach is the investigation of the energy dependence of the stationary wavefunctions, or equivalently, the energy dependence of the wavefunction's phase shift. The latter method, which is widely exploited in

quantum theory of scattering (see [1]), is especially interesting due to the abrupt phase drop, equal to π, in a very narrow energy range around every quasi-discrete resonance (see Figs. 9 and 10 in [12]).

In this paper the quasi-bound levels are fixed as the maxima of the wavefunction $\Psi(E, LTP)$ depending on energy, with $R = LTP(E)$ being the solutions of the equation $E = U(R)$ in the range $R < R_1$, that is, the left classical turning points (LTP) for the potential. If $LTP \leq X_1$, one directly finds the maximum of the function $\Psi_0(E) = C_0(E, LTP) \cos[\varphi_0(E) + D_0(E, LTP) - \alpha_0 \beta_0(E) LTP]$ according to (10). In case $LTP > X_1$, one first uses the conditions $\Psi_0(E, X_1) = \Psi_{11}(E, X_1)$ and $F_0(E, X_1) = F_{11}(E, X_1)$ to fix the constants N_{11} and φ_1 (taking, for example, $N_0 = 1$), and then finds the maximum of the function $\Psi_{11}(E)$ at $R = LTP(E)$ according to (24). To reduce the amount of calculations for ascertaining the quasi-bound resonant states, one again needs good initial prognoses for these quasi-discrete levels. Fortunately, formula (30) serves for this purpose as well. Having fixed a quasi-bound state $E = E_n$, one uses the conditions $\Psi_{11}(E_n, X_2) = \Psi_{22}(E_n, X_2)$ and $F_{11}(E_n, X_2) = F_{22}(E_n, X_2)$ to find the actual values of the normalization factors N_0, N_{11}, and the phase shift φ_2 in (10), (24), and (26). Naturally, the same procedure can be performed for any energy (i.e., not necessarily for the resonances' maxima) $E \geq V_2 + D_2$ if one is interested in the corresponding stationary wavefunction.

The results of calculations are presented in Figs. 4–6. They are all related to the effective potential curve for the rotationally excited xenon excimer, which is demonstrated in Fig. 4 (where the pseudo-Morse component is not seen, since it surpasses the bounds of the figure). One can see that due to the extreme narrowness of the lower resonances there is actually no distinct border between bound and quasi-bound states. For example, to calculate the exact profile of the lowest resonance, all 55 (and even more!) decimal places for its maximum on the upper graph in Fig. 5 should be correct. Apart from the obvious fact that one never could fix any potential with such an accuracy, the lifetime of this resonance (speaking in terms of the quasi-stationary states) would be of the order of 10^{32} years, that is, much more compared with the age of the Universe. This extraordinary result simply means that there is no need to associate the lower resonances with the continuous energy spectrum: in any practical application they can be treated as usual bound states. Such a claim can be extended to all quasi-bound levels up to the second highest, and with some caution, even to the highest resonance, as can be inferred from Fig. 5.

Figure 6 demonstrates that there is actually no need for a high computer precision to accurately ascertain the stationary wavefunction related to a quasi-bound level. Indeed, if the maximum of the lowest resonance is fixed with only 9 decimal places, the wavefunction's actual amplitude in the metastability range $(R < R_2)$ diminishes by a factor of 1.3409×10^{47}, thus becoming invisible in its asymptotic free wave's scale (the lower graph in Fig. 6). In spite of this as if enormous effect the shape of the wavefunction in the metastability range practically
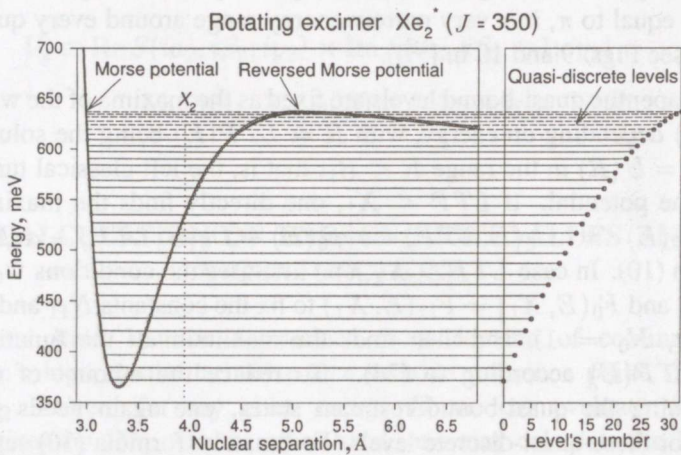
Fig. 4. An exactly solvable (solid line on the left graph) substitute potential (dots representing the original potential) for the rotating xenon excimer in the 0_u^+ state. The positions of the bound (solid horizontal lines) and quasi-bound (dashed lines) levels are also shown.
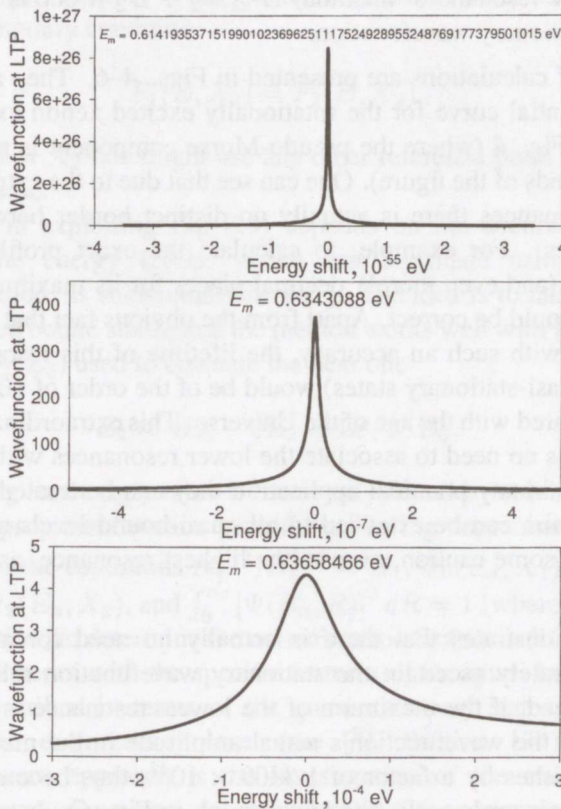

Fig. 5. The profiles of the resonances (the lowest and the two highest) for the rotating ($J = 350$) excimer Xe_2^* (0_u^+).
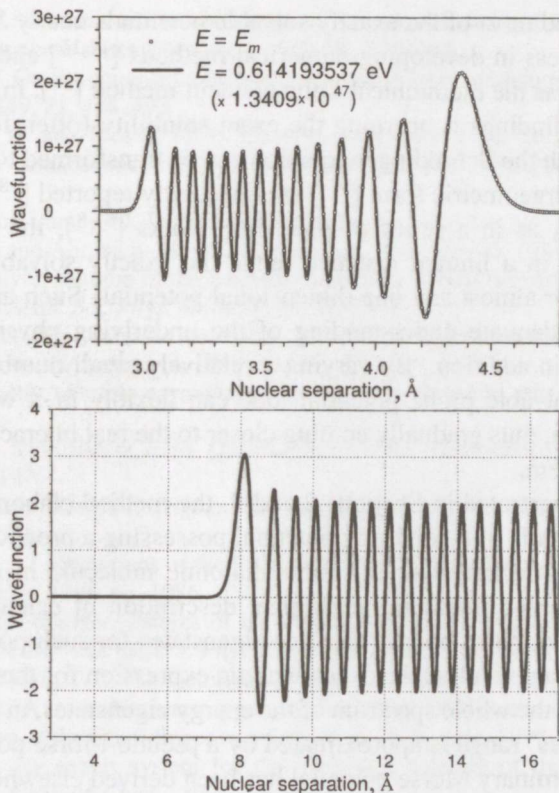
246

Fig. 6. Two different wavefunctions related to the lowest quasi-bound state shown on the upper graph in Fig. 5. One of them (dots) has been calculated for the exact maximum position (with more than 55 decimal places needed to fix it), while the other (solid line) has been fixed with the precision of only 9 decimal places. The lower graph represents the free wave's part of the latter wavefunction.

does not change, compared with that for the exact maximum position. Therefore, even when calculated with the considerably reduced precision, the wavefunction can be normalized within the range $R \in (0, R_2)$, and one needs not worry about the formally quasi-bound nature of the level. This way the computation time for determining the whole spectrum of the bound and quasi-bound states can be dramatically decreased.

4. CONCLUSION

The problem of the exact solubility of the one-dimensional Schrödinger equation has attracted and inspired theorists since the advent of quantum mechanics. The interest in this subject has not fallen off, although Infeld and

Hull [13] classified most of the exactly solvable potentials nearly 50 years ago, and despite the progress in developing numerical methods [14,15] and fascinating new techniques, such as the hierarchical finite element method [16], in the recent years. New theoretical findings concerning the exact solubility (often formulated as the problem for which the Schrödinger equation can be transformed to hypergeometric or confluent hypergeometric form [17]) are constantly reported [18−20].

In this paper, as in a series of preceding works [6−8], the author aimed to demonstrate that in a limited distance range the exactly solvable substitute can be constructed for almost any one-dimensional potential. Such an approach leads one to a more adequate understanding of the underlying physics, giving some aesthetic appeal in addition. By varying a relatively small number of parameters for an exactly solvable probe potential, one can flexibly fit it with the available experimental data, thus gradually coming closer to the real interaction potential for the quantum system.

As was demonstrated in Sections 2 and 3, the method elaborated can be used to examine all details of a confining potential possessing a pronounced maximum, for example, an effective potential for a diatomic molecule in a high rotational substate. The unified quantum-mechanical description of calculating the whole spectrum of bound, quasi-bound, and free eigenstates for such potentials has been given. An important result is the exact analytic expression for the phase shift (12), which is valid for the whole spectrum of the energy eigenstates, in presumption that the small distances' range is approximated by a pseudo-Morse potential (a similar formula for the ordinary Morse potential has been derived elsewhere [8]).

A fundamental problem not touched in this paper is the correct normalization of the wavefunctions in the continuous energy spectrum. As explained in Section 3, this problem practically does not concern the quasi-bound states, except the rather indefinite highest resonance (see the lowest graph in Fig. 6), for which a small correction of the asymptotic normalization (27) might be needful, if one aims at a rigorous description. Indeed, as demonstrated in [7], the asymptotic normalization recommended in handbooks on quantum mechanics is incorrect near the bound of the discrete and continuous spectra, while the relevant correction factor is well described by a Fano line shape function [21].

REFERENCES

1. Chadan, K. and Sabatier, P. C. *Inverse Problems in Quantum Scattering Theory*. Springer, New York, 1977.

2. Bargmann, V. Remarks on the determination of a central field of force from the elastic scattering phase shifts. *Phys. Rev.*, 1949, **75**, 301–302.

3. Bargmann, V. On the connection between phase shifts and scattering potential. *Rev. Mod. Phys.*, 1949, **21**, 488–493.

4. Abraham, P. B. and Moses, H. E. Changes in potentials due to changes in the point spectrum: anharmonic oscillators with exact solutions. *Phys. Rev. A*, 1980, **22**, 1333–1340.

5. Luban, M. and Pursey, D. L. New Schrödinger equations for old: inequivalence of the Darboux and Abraham–Moses constructions. *Phys. Rev. D*, 1986, **33**, 431–436.

6. Selg, M. Analytic solution of the stationary one-dimensional Schrödinger equation. *Proc. Estonian Acad. Sci. Phys. Math.*, 1998, **47**, 29–47.

7. Selg, M. Exactly solvable modified Morse potentials for quantum-mechanical applications. *Phys. Scripta*, 1999, **60**, 491–500.

8. Selg, M. Exactly solvable asymmetric double-well potentials. *Phys. Scripta*, 2000, **62**, 108–116.

9. Landau, L. D. and Lifshitz, E. M. *Quantum Mechanics-Nonrelativistic Theory*. Pergamon, Oxford, 1976.

10. Bateman, H. and Erdélyi, A. *Higher Transcendental Functions*, Vol. 1. McGraw-Hill, New York, 1953.

11. Chebotarev, L. V. Extensions of the Bohr–Sommerfeld formula to double-well potentials. *Am. J. Phys.*, 1998, **66**, 1086–1095.

12. Selg, M. Quasi-discrete features of the continuous energy spectrum: an application to metastable Xe*–Xe pairs. *J. Phys. B: At. Mol. Opt. Phys.*, 1996, **29**, 699–713.

13. Infeld, L. and Hull, T. E. The factorization method. *Rev. Mod. Phys.*, 1951, **23**, 21–68.

14. Simos, T. E. A new Numerov-type exponentially fitted method for the numerical integration of the Schrödinger equation. *Helv. Phys. Acta*, 1999, **72**, 1–22.

15. Simos, T. E. An expert system for the numerical solution of the radial Schrödinger equation. *Comput. Chem.*, 1999, **23**, 1–7.

16. Sugawara, M. Adaptive basis set for quantum mechanical calculation based on hierarchical finite element method. *Chem. Phys. Lett.*, 1998, **295**, 423–430.

17. Cooper, F., Ginocchio, J. N. and Khare, A. Relationship between supersymmetry and solvable potentials. *Phys. Rev. D*, 1987, **36**, 2458–2473.

18. Junker, G. Conditionally exactly solvable potentials: a supersymmetric construction method. *Ann. Phys.*, 1998, **270**, 155–177.

19. Rosas-Ortiz, J. O. Exactly solvable hydrogen-like potentials and the factorization method. *J. Phys. A: Math. Gen.*, 1998, **31**, 10163–10179.

20. Chuan, C. X. Higher order generation of exactly solvable supersymmetric systems. *Int. J. Theor. Phys.*, 1999, **38**, 745–756.

21. Fano, U. Effects of configuration interaction on intensities and phase shifts. *Phys. Rev.*, 1961, **124**, 1866–1878.

TÄPSELT LAHENDUV MAKSIMUMI OMAV POTENTSIAAL

Matti SELG

Ühedimensioonilise Schrödingeri võrrandi lahendamiseks väljatöötatud üldist analüütilist meetodit on rakendatud potentsiaalidele, mille koordinaadisõltuvuse maksimumväärtus ületab tunduvalt piirväärtust lõpmatuses. Meetodi põhiidee

on konstrueerida etteantud lähtepotentsiaali võimalikult täpselt lähendav ning samas täpselt lahenduv asenduspotentsiaal, mis koosneb mitmest omavahel sujuvalt ühendatud Morse tüüpi (hariliku, ümberpööratud või pseudo-Morse) komponendist. Töös on antud täielik ülevaade kõigist analüütilistest protseduuridest, mis on vajalikud kõnealuse kvantsüsteemi seotud ja kvaasiseotud seisundite spektri ning vastavate statsionaarsete lainefunktsioonide arvutamiseks. Lisaks sellele on tuletatud täpne valem lainefunktsiooni asümptootilist käitumist määrava faasinihke parameetri arvutamiseks suvalise energiaväärtuse korral. Meetodi tulemuslikkust on demonstreeritud kõrges pöörlemisseisundis asuva ksenooni eksimeeri näitel.